

## Research Article

# Numerical Simulation of an Industrial Absorber for Dehydration of Natural Gas Using Triethylene Glycol

**Kenneth Kekpugile Dagde and Jackson Gunorubon Akpa**

*Department of Chemical/Petrochemical Engineering, Rivers State University of Science & Technology, Nkpolu, Port Harcourt, Rivers State, Nigeria*

Correspondence should be addressed to Kenneth Kekpugile Dagde; kenneth\_dagde@yahoo.com

Received 27 May 2014; Accepted 24 June 2014; Published 20 July 2014

Academic Editor: Hyun Seog Roh

Copyright © 2014 K. K. Dagde and J. G. Akpa. This is an open access article distributed under the Creative Commons Attribution License, which permits unrestricted use, distribution, and reproduction in any medium, provided the original work is properly cited.

Models of an absorber for dehydration of natural gas using triethylene glycol are presented. The models were developed by applying the law of conservation of mass and energy to predict the variation of water content of gas and the temperature of the gas and liquid with time along the packing height. The models were integrated numerically using the finite divided difference scheme and incorporated into the MATLAB code. The results obtained agreed reasonably well with industrial plant data obtained from an SPDC TEG unit in Niger-Delta, Nigeria. Model prediction showed a percentage deviation of 8.65% for gas water content and 3.41% and 9.18% for exit temperature of gas and liquid, respectively.

## 1. Introduction

Natural gas needs to be dried before pipeline transport, because the water molecules present in the gas in both vapour and liquid state form hydrates which cause flow restrictions and pressure drops and lower the heating value of gas and corrode pipelines and other equipment. Other problems associated with the presence of water molecules are foaming, degradation, puking, corrosion, low pH, oxidation, thermal decomposition, inadequate absorber design for flow conditions, and salt contamination. Extensive literature is available on common gas dehydration systems including solid and liquid desiccant and refrigeration-based systems [1, 2]. There are several methods of dehydrating natural gas. The most common of these are liquid desiccant (glycol) dehydration and solid desiccant dehydration [3, 4]. Among these gas dehydration processes, absorption is the most common technique, where the water vapor in the gas stream becomes absorbed in a liquid solvent stream. Glycols are the most widely used absorption liquids as they approximate the properties that meet commercial application criteria [5, 6]. Several glycols have been found suitable for commercial application. Triethylene glycol (TEG) is by far the most common liquid desiccant used in natural gas dehydration

as it exhibits most of the desirable criteria of commercial suitability [2]. The glycol absorber (contactor) contains trays that provide an adequate intimate contact area between the gas and the glycol. One other option to the tray TEG contactor is the use of structured packing. Structured packing was developed as an alternative to random packing to improve mass transfer control by use of a fixed orientation of the transfer surface. The combination of high gas capacity and reduced height of an equilibrium stage, compared with tray contactors, makes the application of structured packing desirable for both new contactor designs and existing tray contactor capacity upgrades. Hence, the structured packing may offer potential cost savings over trays [1].

Optimization of glycol dehydration unit of a natural gas plant is generally aimed at developing a suitable mathematical model which, when tested with plant data, will aid in deciding the best operating conditions required to reduce natural gas water content to the standard pipeline specification of less than 7 lb H<sub>2</sub>O/MMSCF of gas [7, 8]. Triethylene glycol (TEG) would be used as the absorbent for this process and would be regenerated in a glycol dehydration unit to 99% purity. This, however, is not the case in most of these units. Jaćimović et al. [9] simulated a reactive absorption system for the absorption of CO<sub>2</sub> in a packed column using methyl diethanolamine

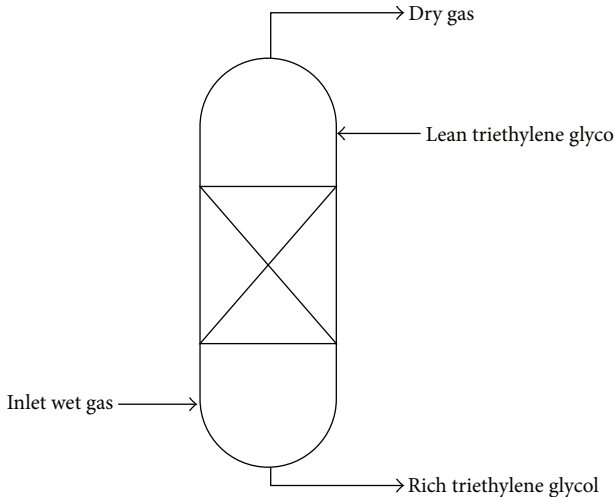


FIGURE 1: Schematic of the dehydrator.

(MDEA) as the solvent. Steady state conditions and plug flow were assumed for the gas phase, leading to a set of ordinary differential equations. In Richardson et al. [10], a mathematical model for the wet scrubbing of  $\text{CO}_2$  using chilled ammonia was studied. Diffusion and conduction terms were included in the development of the unsteady state models. These models predict the variation of the concentration of the reactants and products with time across the packed height, as well as the variation of the temperature of the system with time across the packed height. The partial differential equations developed were solved using the numerical technique of MATLAB by applying the Robin, Neumann, and Dirichlet boundary conditions (BC) [11]. A similar study on  $\text{CO}_2$  absorption was carried out by Ahmed et al. [12] using a highly concentrated monoethanolamine (MEA). Most studies on gas dehydration using TEG were simulated using special packages like HYSYS used by Peyghambarzadeh and Jafarpour [13] and the parameters used in their models cannot be easily obtained without extensive experimental studies; thus the model cannot be adapted for simulation of industrial absorber unit. In this paper, models for a functional industrial absorber are presented. The results from the models are compared with data obtained from functional full-scale industrial absorber plant.

## 2. Model Development

The most common method for dehydration in the natural gas industry is the use of a liquid desiccant contactor (absorber) process. In this process, the wet gas is contacted with lean solvent (triethylene glycol) as the absorbent. The water in the gas is absorbed in the lean solvent, producing a rich solvent stream and a dry gas. The dehydrated gas leaves at the top of the column while the glycol leaves at the bottom. Figure 1 depicts the hypothetical representation of the dehydrator.

The entering wet gas enters the bottom of the absorber and flows up counter currently against the lean triethylene glycol, which enters at the top of the absorber. The triethylene glycol absorbs water vapour from the wet gas as it flows down

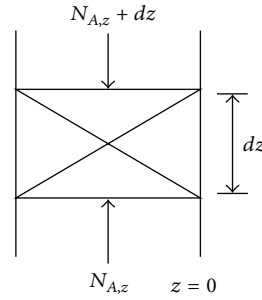


FIGURE 2: Elemental packed volume.

the column and leaves the bottom of the column rich in water, whereas dry gas leaves from the top of the dehydrator. Therefore, the mass diffusion principles governing this operation will be used in developing the mathematical models for the dehydrator. The models would be developed using the principle of conservation of mass and energy to predict the variation of water content in the gas and the variation of temperature of the gas and triethylene glycol across the height of the dehydrator.

## 3. Model Formulation/Assumptions

The following assumptions were made to develop the model.

- (i) Since the column requirement is a diameter  $\leq 0.65$  m, a packing height of  $\leq 6$  m and the fluid are corrosive coupled with a minimum pressure drop across the column, and packed column is preferred to plate column [14, 15].
- (ii) The absorber is well lagged; hence, the heat losses are negligible.
- (iii) Since the water vapour in the wet gas is the only diffusing component, no diffusing term would be considered for the liquid phase.
- (iv) The effect of change in total molar flow rate is ignored, and an average value is assumed constant [16, 17].
- (v) Vapour-liquid equilibrium relationship is described using Raoult's law and Antoine's equation used for calculation of vapour pressure [18].

**3.1. Model Development.** Material balance (gas phase): Figure 2 shows the elemental packed volume and its flow.

Consider a homogeneous medium consisting of wet gas ( $A$ ) and nondiffusive triethylene glycol ( $B$ ). Let the packed bed be stationary (i.e., the molar average velocity of the mixture is zero), and the mass transfer may occur only by diffusion.

Now consider a differential control volume  $dx dy dz$ .

**3.1.1. Mass Balance.** A general equation can be derived for a binary mixture of wet gas and nondiffusive triethylene glycol for diffusion and convection that also includes terms for unsteady-state diffusion and chemical reaction. Making the

material balance on the wet gas on an element of  $dx$ ,  $dy$ , and  $dz$  fixed in space and shown in Figure 2,

$$-\left[ \frac{\partial}{\partial x} (N_{A,x}) + \frac{\partial}{\partial y} (N_{A,y}) + \frac{\partial}{\partial z} (N_{A,z}) \right] = \frac{\partial C_A}{\partial t}. \quad (1)$$

For a packed column that is, stationary media, applying Fick's law (1) reduces to

$$\begin{aligned} -\left[ \frac{\partial}{\partial x} \left( D_{AB} \frac{\partial C_A}{\partial x} \right) + \frac{\partial}{\partial y} \left( D_{AB} \frac{\partial C_A}{\partial y} \right) + \frac{\partial}{\partial z} \left( D_{AB} \frac{\partial C_A}{\partial z} \right) \right] \\ = \frac{\partial C_A}{\partial t}. \end{aligned} \quad (2)$$

If  $D_{AB}$  is constant, (2) becomes

$$-\left[ \frac{\partial^2 C_A}{\partial x^2} + \frac{\partial^2 C_A}{\partial y^2} + \frac{\partial^2 C_A}{\partial z^2} \right] = \frac{1}{D_{AB}} \frac{\partial C_A}{\partial t}. \quad (3)$$

Since the absorber is in vertical position,

$$-\frac{d^2 C_A}{\partial x^2} = \frac{\partial^2 C_A}{\partial y^2} = 0. \quad (4)$$

Equation (3) now becomes

$$\frac{\partial^2 C_A}{\partial z^2} = \frac{1}{D_{AB}} \frac{\partial C_A}{\partial t}. \quad (5)$$

But

$$C_A = C_{AO} (1 - y_A). \quad (6)$$

Differentiating (6),

$$dC_A = -C_{AO} dy_A, \quad (7a)$$

$$d^2 C_A = -C_{AO} d^2 y_A. \quad (7b)$$

Substituting (7a) and (7b) into (5) gives

$$\frac{\partial y_A}{\partial t} = D_{AB} \frac{\partial^2 y_A}{\partial z^2}. \quad (8)$$

The model equation (8) can be used to predict the variation of water content of gas along the column height at different residence times.

**3.1.2. Energy Balance.** The energy balance will be carried out using the principle of conservation of energy for both the gas and the liquid triethylene glycol. The glycol enters the column at a higher temperature, transferring some amount of heat to the gas, and hence gas phase energy balance is included.

**3.1.3. Energy Balance for the Gas Phase.** Figure 3 depicts the hypothetical representation of the differential element for energy balance of the gas phase within the packing height, where  $T_{og}$  and  $T_g$  are the inlet and outlet temperature of the gas,  $q_z$  and  $dq_z$  are the inlet quantity of heat and outlet

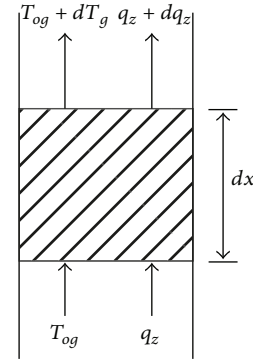


FIGURE 3: Hypothetical representation of the energy balance within the differential packing height.

quantity of heat from the packing space ( $dq_z$ ), and  $dz$  is the incremental height of the packing space.

Taking cognizance of the conduction of heat axially up the column due to molecular diffusion, the energy balance of the differential element applying the conservation principle gives

$$\frac{\partial T_g}{\partial t} = \frac{\dot{m}}{AC_{Ag}} \frac{\partial T_g}{\partial z} + \frac{K_g \partial^2 T_g}{C_{Ag} C_{Pg} \partial z^2} + \frac{Q}{Adz C_{Ag} C_{Pg}}, \quad (9)$$

where  $C_{Pg}$  is the specific capacity of water vapour in the gas stream,  $q_z$  is the heat flux in the  $z$ -direction due to molecular conduction by Fourier's law,  $A$  is the area of the packing space, and  $Q$  is the amount of heat transferred from the lost glycol to the gas steam. The heat transfer at constant pressure is given by Vuthaluru and Bahadori [19] as

$$Q = LC_{PL} dT_L, \quad (10)$$

where  $L$  is the molar flow rate of triethylene glycol in mol/s and  $C_{PL}$  and  $dT_L$  are the heat capacity and temperature difference of the liquid glycol.

Recall from dimensional analysis that

$$\frac{k_g}{C_{Ag} C_{Pg}} = \alpha_g, \quad (11)$$

where  $\alpha_g$  is the thermal diffusivity of water vapour in  $\text{m}^2/\text{s}$ .

Substituting (10) and (11) into (9) results into

$$\frac{\partial T_g}{\partial t} = -\frac{\dot{m}}{AC_{Ag}} \frac{\partial T_g}{\partial z} + \alpha \frac{\partial^2 T_g}{\partial z^2} + \frac{LC_{PL}}{AC_{Ag} C_{Pg}} \frac{\partial T_L}{\partial z}. \quad (12)$$

Let  $\gamma = -\dot{m}/AC_{Ag}$  and  $\beta = (LC_{PL}/AC_{Ag} C_{Pg})(\partial T_L/\partial z)$ , giving

$$\frac{\partial T_g}{\partial t} = \gamma \frac{\partial T_g}{\partial z} + \alpha \frac{\partial^2 T_g}{\partial z^2} + \beta. \quad (13)$$

**3.1.4. Energy Balance for the Liquid Phase.** Figure 4 depicts the hypothetical representation of the inlet and outlet flow into and out from the differential packing bed in the column.

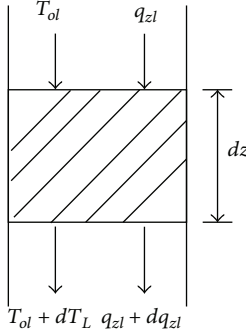


FIGURE 4: Schematic energy balance for liquid phase.

TABLE 1: Inlet conditions [20].

Components	Input streams			
	Gas stream		Glycol stream	
	Weight %	Mol %	Weight %	Mol %
TeG	—	—	99.51	96.054
H <sub>2</sub> O	0.17	0.187	0.49	3.946
Gas	99.83	99.813	—	—
Total	<b>100.00</b>	<b>100.00</b>	<b>100.00</b>	<b>100.00</b>
Temperature °C	50		55	

Similarly the energy balance for the liquid phase is made using the principles of conservation of energy taking cognizance that the triethylene glycol flows from the top to the bottom of the column to obtain

$$\frac{\partial T_L}{\partial t} = \frac{-\dot{m}_L}{AC_{AL}} \frac{\partial T_L}{\partial z} + \alpha_L \frac{\partial T_L^2}{\partial z^2}, \quad (14)$$

where  $\alpha_L = k_L/C_{AL}C_{PL}$  is the thermal diffusivity in the liquid phase (triethylene glycol) in  $\text{m}^2/\text{s}$ .

Equations (8), (13), and (14) constitute the mass balance for the water content in feed gas and the energy balances for gas temperature and TEG temperature variations, respectively, in the absorber.

### 3.2. Operational Parameter and Solution Techniques

**3.2.1. Operational Parameters.** The input and output operating conditions and the physical properties of the wet gas and glycol (density, molecular weight, and molar volume mass and thermal diffusivity) were estimated from an industrial plant [3, 20] and are presented in Tables 1, 2, and 3.

**Empirical Evaluation of Mass Diffusivity.** The mass diffusivity of water vapour in triethylene glycol (TEG) is evaluated using the formula [3, 21]

$$D_{12} = 1.1728 \times 10^{-16} T \frac{(x^2 M^2)^{1/2}}{\mu_2 V_1^{0.6}}, \quad (15)$$

TABLE 2: Outlet conditions [20].

Components	Output streams			
	Gas stream		Glycol stream	
	Weight %	Mol %	Weight %	Mol %
TeG	—	—	95.36	71.127
H <sub>2</sub> O	0.01	0.011	4.04	28.873
Gas	99.99	99.989	—	—
Total	<b>100.00</b>	<b>100.00</b>	<b>100.00</b>	<b>100.00</b>
Temperature °C	51.3			51

TABLE 3: Physical properties of components [3].

Properties	TEG	H <sub>2</sub> O	GAS
Molar mass	150.17	18.02	19.83
Molar volume, $\text{m}^3/\text{Kmol}$	0.01813	—	—
Mass diffusivity, $\text{m}^2/\text{s}$	$3.80 \times 10^{-10}$	—	—
Thermal diffusivity, $\text{m}^2/\text{s}$	$2.338 \times 10^{-5}$	—	—
Density, $\text{Kg/m}^3$	1125	1000	—

where subscript 1 represents the water vapour in the gas, and subscript 2 represents triethylene glycol, where  $T = 50^\circ\text{C} = 323.15 \text{ K}$  and at  $T = 50^\circ\text{C}$ ,  $\mu_2 = 0.01355515 \text{ Pa}\cdot\text{sec}$ .

**Solvent Association Parameters.**  $X_2 = 1$  for (TEG),  $V_1 = 0.0183 \text{ m}^3/\text{Kmol}$ , and  $M_2 = 150.17 \text{ Kg/Kmol}$ .

Substitution of these values into (15) gives

$$D_{12} = 3.80 \times 10^{-10} \text{ m}^2/\text{s}. \quad (16)$$

**Inlet Gas and Glycol Water Content.** The inlet gas and glycol water content (in weight %) were obtained from plant operating data and were analytically converted to mol% (assuming binary mixture) using the relations. Consider

$$y_1 = \frac{x_1/m_1}{x_1/m_1 + x_2/m_2}, \quad (17)$$

$$y_2 = 1 - y_1,$$

where  $x_1$  and  $x_2$  are concentrations of gas and glycol in wt.%, respectively,  $y_1$  and  $y_2$  are their respective mol%, and  $m_1$  and  $m_2$  are their molecular weight.

**3.2.2. Solution Techniques.** A numerical solution based on the finite divided difference scheme was developed and keyed into MATLAB program to solve the condensed models for gas water content, gas temperature, and TEG temperature variations given in (8), (13), and (14), respectively.

The developed finite divided difference schemes yield finite grids and computational stencils representing the  $y_A$ ,  $T_g$ , and  $T_L$ , from which Boundary conditions were specified according to “Dirichlet BC.” These boundary conditions and initial conditions are given below.

For the gas water content model,

$$\begin{aligned} y_A(z_o, t) &= y_{Ao}, \quad \text{that is, for } z = z_o = 0, 0 \leq t \leq t_m, \\ y_A(z_n, t) &= y_{Af}, \quad \text{that is, for } z = z_n = H, 0 \leq t \leq t_m, \end{aligned} \quad (18)$$

where  $y_{Ao}$  and  $y_{Af}$  are initial and final water content in gas stream, respectively.

The above boundary conditions explain that the initial gas water content is fixed at the inlet point of absorber column ( $z = 0$ ) and change with varying values of residence time ranging from 0 to  $t_m$ . More so, the final gas water content is established at the outlet point of the absorber column ( $z = H$ ) for changing residence time values ranging from 0 to  $t_m$ .

The initial condition is

$$y_A(z, t_o) = 0, \quad \text{that is, for } t = t_o = 0, 0 \leq z \leq H. \quad (19)$$

This implies that the gas water content is established at only zero residence time for varying absorber column height ranging from bottom to top of column.

For the gas temperature model,

$$\begin{aligned} T_g(z_o, t) &= T_{gi}, \quad \text{that is, for } z = z_o = O, 0 \leq t \leq t_m, \\ T_g(z_n, t) &= T_{go}, \quad \text{that is, for } z = z_n = H, 0 \leq t \leq t_m, \end{aligned} \quad (20)$$

where  $T_{gi}$  and  $T_{go}$  are inlet and outlet gas temperatures, respectively.

The above boundary conditions explain that the initial gas temperature is fixed at the inlet point of absorber column ( $z = 0$ ) and changes with varying values of residence time ranging from 0 to  $t_m$ . More so, the final gas temperature is established at the outlet point of the absorber column ( $z = H$ ) for changing residence time values ranging from 0 to  $t_m$ .

The initial condition is

$$T_g(z, t_o) = 0, \quad \text{that is, for } t = t_o = 0, 0 \leq z \leq H. \quad (21)$$

This implies that the gas temperature is established at only zero residence time for varying absorber column height ranging from bottom to top of column.

For the TEG temperature model,

$$\begin{aligned} T_L(z_o, t) &= T_{Li}, \quad \text{that is, for } z = z_o = 0, 0 \leq t \leq t_m, \\ T_L(z_n, t) &= T_{Lo}, \quad \text{that is, for } z = z_n = H, 0 \leq t \leq t_m, \end{aligned} \quad (22)$$

where  $T_{Li}$  and  $T_{Lo}$  are inlet and outlet TEG temperatures, respectively.

The above boundary conditions explain that the initial TEG temperature is fixed at the inlet point of absorber column ( $z = 0$ ) and changes with varying values of residence time ranging from 0 to  $t_m$ . More so, the final TEG temperature is established at the outlet point of the absorber column ( $z = H$ ) for changing residence time values ranging from 0 to  $t_m$ .

The initial condition is

$$T_L(z, t_o) = 0, \quad \text{that is, for } t = t_o = 0, 0 \leq z \leq H. \quad (23)$$

TABLE 4: Comparison between plant data and model predictions.

Process parameter	Model prediction	Plant data	% deviation
Final gas water content	$7.93 \times 10^{-7}$	$7.24 \times 10^{-7}$	8.65
Gas outlet temperature ( $^{\circ}\text{C}$ )	44.52	43	3.41
TEG outlet temperature ( $^{\circ}\text{C}$ )	48.45	44	9.18

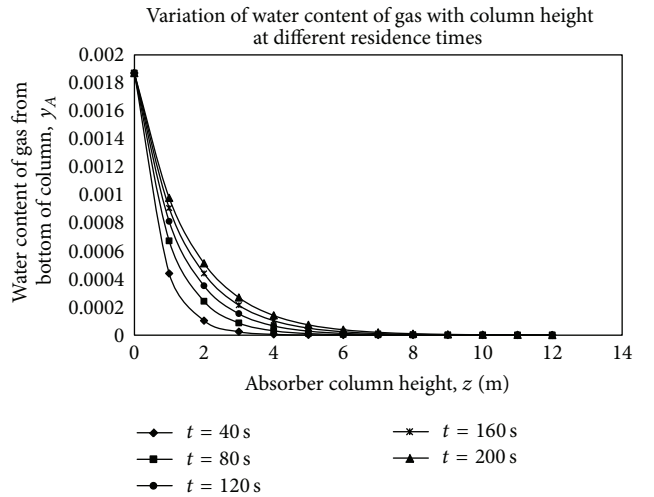


FIGURE 5: Variation of gas water content (mole fraction) from bottom of column.

This implies that the TEG temperature is established at only zero residence time for varying absorber column height ranging from bottom to the top of column.

## 4. Results and Discussion

Table 4 shows the comparison between plant data and predictions from model (see (8), (13), and (14)), indicating that the predicted results agree reasonably well with the plant data. These results show a deviation ranging from 3.41 to 9.18 percent.

Profiles presented and discussed here will subsequently reveal the following: variations of gas water content with time and axial height of packing in the column, variation of temperature of triethylene glycol (TEG) with column height at different thermal diffusivities, variation of temperature of gas with column height at different residence times, variation of gas water content across column height at different mass diffusivities, and variation of temperature of triethylene glycol across the column height at different residence times.

**4.1. Variation of Water Content of Gas with Column Height at Different Residence Times.** It can be deduced from Figure 5 that the water content of the gas reduces as the gas moves from the bottom of the column to the top. It can also be deduced that the higher the residence time of the gas in

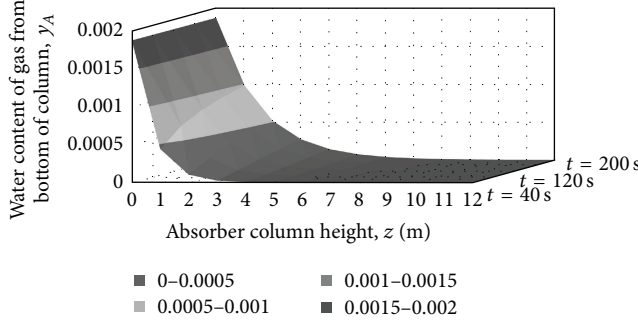


FIGURE 6: Surface plot showing gas water content propagation along the column.

the column, the higher the rate of removal of the water vapour from the gas. This holds true since a relatively smaller time is needed to establish equilibrium between the water vapour in the gas and that in the liquid phase [10, 22]. This means that as the residence time increases, say, to 200 seconds, the water vapour returns to the vapour phase again implying that the water content in gas increases. It can also be deduced from Figure 5 that, at a height of approximately 7 m and above, the gas water content variation becomes steady.

In addition, the solutions of the model will be represented as a three-dimensional surface plot in Figure 6. The purpose of the surface plots is to visualize the propagation of the gas water content in time and space and to make conclusions based on the subsequent trends. The surface plots are not intended to give the exact numerical values but for visualization.

The natural gas propagates from the base of the absorber and initially holds a water concentration of 0.187 mol%. The low resistance in the gas bulk will cause the gas and liquid bulk phases to reach chemical equilibrium virtually instantaneous. The steep transient observed at the lower part of the column confirms the trend illustrated by Figure 6; it is also in agreement with plant data. Also, as operation proceeds half way up the column, the absorption of water from natural gas becomes numerically insignificant and remains practically constant.

**4.2. Variation of Temperature of Triethylene Glycol with the Column Height at Different Residence Times.** In Figure 7, the temperature of the absorbing solvent, triethylene glycol (TEG), reduces gradually as it travels from the top of the column to the bottom. Initially, triethylene glycol enters the column at a temperature of 50°C and leaves at 46.5–48°C depending on the residence time. It is observed that the temperature change becomes smaller as the residence time increases, resulting into a very steep slope at time = 200 seconds. This is obviously because more water vapour has been absorbed at higher residence time.

The surface plot in Figure 8 further visualizes the TEG temperature reduction at varying residence times. The largest TEG temperature change is achieved at a residence time of 40 to 80 seconds, while a little change is achieved at 160 to 200 seconds.

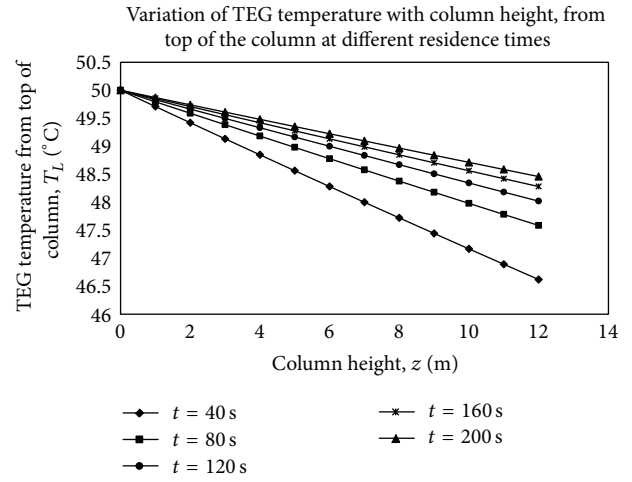


FIGURE 7: Variation of temperature of triethylene glycol down the column.

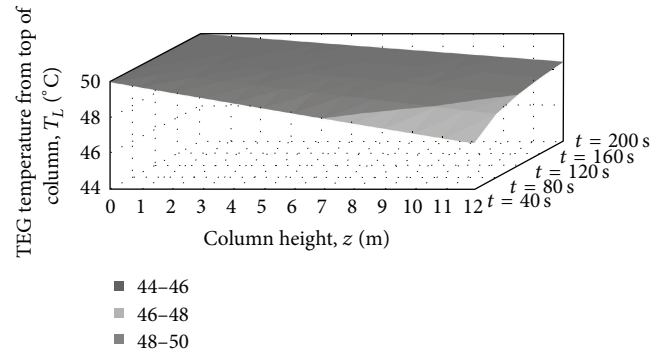


FIGURE 8: Surface plot showing triethylene glycol temperature propagation along the column.

**4.3. Variation of Temperature of Gas with Column Height at Different Residence Times.** The gas enters the column at a temperature of 42.5°C and increases very slowly until it leaves the column at a slightly higher temperature of 46.5°C. However, at a residence time  $t = 40$  seconds and at column height  $z = 12$  m, the outlet temperature of gas is approximately 44.5°C. It can be noticed in Figure 9 that the temperature becomes lower at higher residence time. This implies that if the residence time is reduced further, the required outlet gas temperature would be achieved at approximately 120 seconds. It should be noted that the increase in residence time results from the transfer of heat from the liquid stream to the gas stream.

The surface plot in Figure 10 reveals that the gas temperature variation is not widely distributed. It can be further deduced that the lowest trend in gas temperature is attained at residence time of 120 seconds, while the largest change is obtained at residence time of approximately 40 to 80 seconds.

**4.4. Variation of Water Content of Gas with Column Height at Different Mass Diffusivities.** The mass diffusivity is the property of a material that determines the rate at which a given component is transferred across a concentration

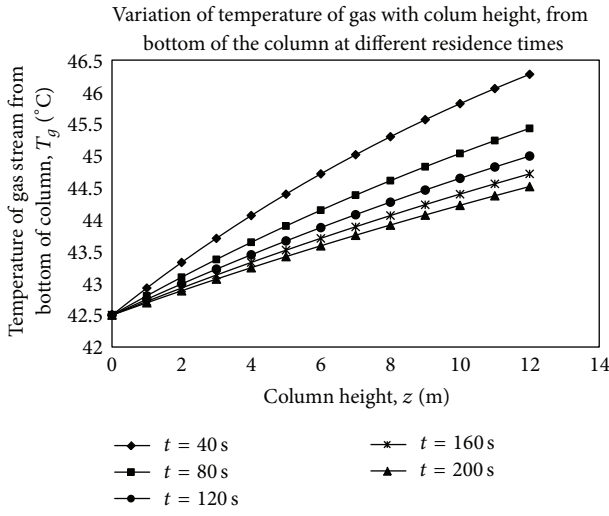


FIGURE 9: Variation of the temperature of the gas stream with column height from column bottom.

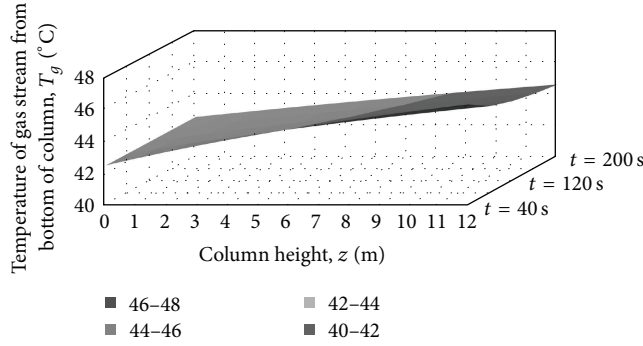


FIGURE 10: Surface plot showing gas temperature variation along the column.

gradient. This property is a vital parameter in this work. From Figure 11, it is evident that, given a fixed time of 40 seconds, at higher mass diffusivities, the rate of transfer of water vapour from gas to the liquid stream decreases slightly as up the column. Also, as the mass diffusivity reduces, the rate of transfer of water vapour from gas to the triethylene glycol stream increases sharply. This implies that the mass diffusion coefficient of the gas through the TEG should be as low as  $\leq 3.80 \times 10^{-10} \text{ m}^2/\text{s}$  for optimal absorption.

The surface plot in Figure 12 shows that the gas water content variation widely spreads across the column height at different mass diffusivities. Similar final gas water content values are obtained at mass diffusivities of  $3.80 \times 10^{-9} \text{ m}^2/\text{s}$  and  $3.80 \times 10^{-10} \text{ m}^2/\text{s}$ .

**4.5. Variation of Temperature of Triethylene Glycol (TEG) with Column Height at Different Thermal Diffusivities.** Thermal diffusivity is the property of a material which describes the rate at which heat flows through the material. Water vapour, being a better heat transfer agent, has a value of  $2.336 \times 10^{-5} \text{ m}^2/\text{s}$ , whereas liquid water has a value of  $1.4 \times 10^{-5} \text{ m}^2/\text{s}$ . From Figure 13, it is observed generally that the temperature

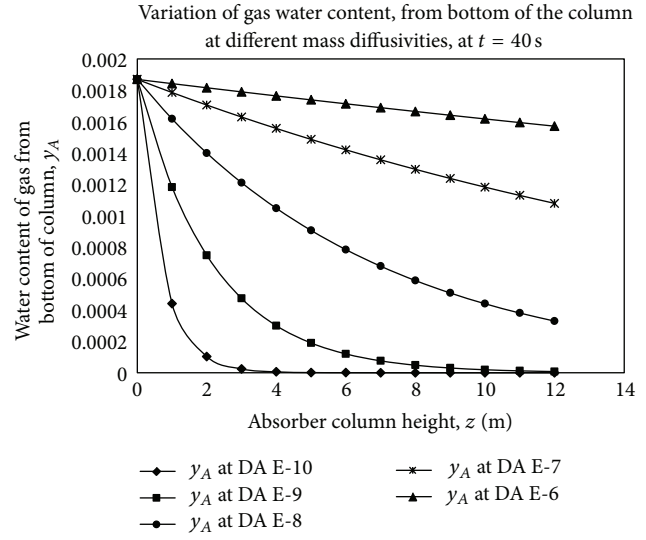


FIGURE 11: Variation of water content of gas at different mass diffusivities at  $t = 40$  seconds.

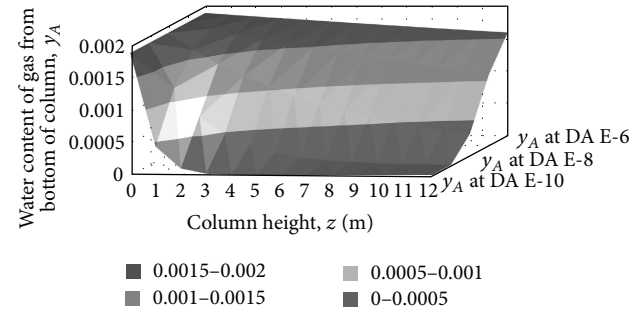


FIGURE 12: Surface plot showing gas water content variation at different mass diffusivities when time = 40 seconds.

of the solvent triethylene glycol decreases sharply down the column as the thermal diffusivity decreases. This decrease is faster as the thermal diffusivity decreases, resulting in a steep slope at the lowest thermal diffusivity of  $2.338 \times 10^{-5} \text{ m}^2/\text{s}$ . It is imperative to note that these plots were taken at a residence time of  $t = 40$  seconds.

In addition, the surface plot in Figure 14 clearly visualizes the TEG temperature decrease along the column and at varying thermal diffusivities. A relatively large TEG temperature change exists between thermal diffusivities of  $2.338 \times 10^{-4}$  and  $2.338 \times 10^{-5} \text{ m}^2/\text{s}$ ; conversely, there is a insignificant temperature change at  $2.338 \times 10^{-1} \text{ m}^2/\text{s}$ .

## 5. Conclusion

Mathematical models of the absorber of a glycol dehydration facility were developed using the principles of conservation of mass and energy. The models could predict the variation of the water content of gas in mole fraction and the gas and liquid (TEG) temperatures across the packing height. The models developed contain contributions from bulk and diffusion flows. The models were validated using the initial

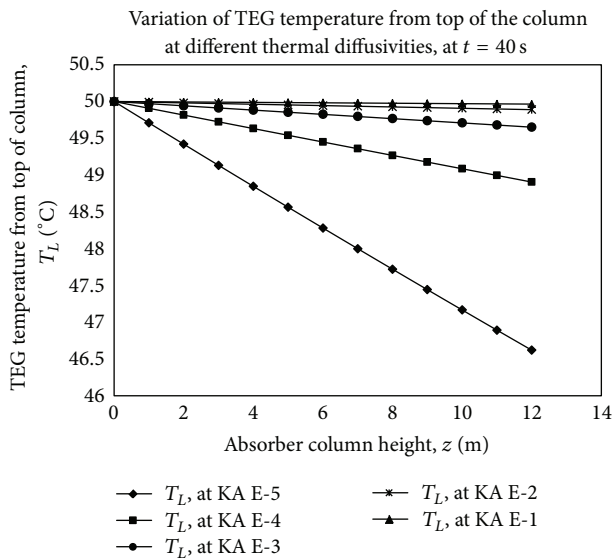


FIGURE 13: Variation of temperature of TEG with thermal diffusivities at  $t = 40$  seconds.

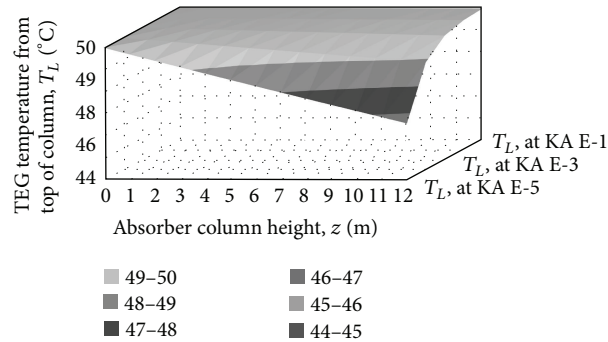


FIGURE 14: Surface plot of TEG temperature at different thermal diffusivities at  $t = 40$  seconds.

conditions from a functional industrial TEG unit in Nigeria to ascertain if the outlet conditions predicted by the models meet the industrial plant outlet values.

## Conflict of Interests

The authors declare that there is no conflict of interests regarding the publication of this paper.

## References

- [1] J. M. Campbell, R. N. Maddox, L. F. Sheerar, and J. H. Erbar, *Gas Conditioning and Processing*, vol. 3 of *Campbell Petroleum Series*, Campbell Petroleum, Norman, Okla, USA, 1982.
- [2] J. M. Campbell, *Gas Conditioning and Processing*, vol. 2, Campbell Petroleum Series, Norman, Okla, USA, 7th edition, 1992.
- [3] R. H. Perry and D. W. Green, *Perry's Chemical Engineers' Handbook*, McGraw Hil, New York, NY, USA, 7th edition, 1999.
- [4] N. A. Darwish and N. Hilal, "Sensitivity analysis and faults diagnosis using artificial neural networks in natural gas TEG-dehydration plants," *Chemical Engineering Journal*, vol. 137, no. 2, pp. 189–197, 2008.
- [5] A. Bahadori, H. B. Vuthaluru, and S. Mokhatab, "Analyzing solubility of acid gas and light alkanes in triethylene glycol," *Journal of Natural Gas Chemistry*, vol. 17, no. 1, pp. 51–58, 2008.
- [6] A. Bahadori and H. B. Vuthaluru, "Simple methodology for sizing of absorbers for TEG (triethylene glycol) gas dehydration systems," *Energy*, vol. 34, no. 11, pp. 1910–1916, 2009.
- [7] C. U. Ikoku, *Natural Gas Production Engineering*, Kreiger Publishing, Malabar, Fla, USA, 1992.
- [8] Gas Processors Suppliers Association (GPSA), *Engineering Data Book*, chapter 20, Gas Processors Suppliers Association, Tusla, Okla, USA, 11th edition, 1998.
- [9] B. M. Jaćimović, S. B. Genić, D. R. Djordjević, N. J. Budimir, and M. S. Jarić, "Estimation of the number of trays for natural gas triethylene glycol dehydration column," *Chemical Engineering Research and Design*, vol. 89, no. 6, pp. 561–572, 2011.
- [10] J. F. Richardson, J. H. Harker, and J. R. Backhurst, *Coulson & Richardson's Chemical Engineering: Chemical Engineering Design*, vol. 6, Elsevier, New Delhi, India, 3rd edition, 2002.
- [11] S. Chapra and R. P. Canale, *Numerical Methods for Engineers*, McGraw Hill International Edition, 6th edition, 2009.
- [12] A. Ahmed, T. Paitoon, and I. Raphael, *Chemindex*, ccu/09, International Test Centre for Carbon Dioxide Capture (ITC), Faculty of Engineering, University of Regina, Regina, Canada, 2007.
- [13] S. M. Peyghambarzadeh and M. Jafarpour, "Impact of thermodynamic model on the simulation of natural gas dehydration unit," in *Proceedings of the 6th National-Student Chemical Engineering Congress*, pp. 1–10, University of Isfahan, 2006.
- [14] S. Max, D. T. Klaus, and E. W. Ronald, *Plant Design and Economics for Chemical Engineers*, McGraw Hill International, New York, NY, USA, 5th edition.
- [15] L. Mei and Y. J. Dai, "A technical review on use of liquid-desiccant dehumidification for air-conditioning application," *Renewable and Sustainable Energy Reviews*, vol. 12, no. 3, pp. 662–689, 2008.
- [16] W. L. McCabe, J. Smith, and P. Harriott, *Unit Operations of Chemical Engineering*, McGraw-Hill, New York, NY, USA, 7th edition, 2005.
- [17] D. M. Himmelblau, *Basic Principles and Calculate in Chemical Engineering*, Prentice-Hall, New Delhi, India, 6th edition, 2005.
- [18] Y. S. Choe, *Regrowns dynamic models of distillation columns* [M.S. thesis], Lehigh University, Bethlehem, Pa, USA, 1985.
- [19] H. B. Vuthaluru and A. Bahadori, "A new method for prediction of absorption/stripping factor," *Computer and Chemical Engineering*, vol. 34, pp. 1731–1736, 2010.
- [20] Shell Petroleum Development Company (SPDC) of Nigeria, "Gbaran Ubie Integrated Oil & Gas Development Project, Gas Dehydration & Glycol Regeneration Packages," Operating Manual, 2007.
- [21] P. Gandhidasan and A. A. Al-Mubarak, "Dehydration of natural gas using solid desiccants," *Energy*, vol. 26, no. 9, pp. 855–868, 2001.
- [22] J. F. Richardson, J. H. Harker, and J. R. Backhurst, *Coulson & Richardson's Chemical Engineering: Particle Technology and Separation Process*, vol. 2, Elsevier, New Delhi, India, 5th edition, 2002.

